DELPHI Collaboration DELPHI 97-165 PHYS 742
14 October, 1997

Search for the decay $\tilde{\tau} \to \tau \tilde{G}$, in the framework of Minimal Gauge Mediated SUSY Breaking models.

F.R. Cavallo and F.L. Navarria
INFN Bologna and Bologna University, Viale Berti Pichat 6/2, I-40126 Bologna

Abstract

A search for $\tilde{\tau} \to \tau \tilde{G}$ decays was carried out, in the context of Gauge Mediated SUSY Breaking models, using the data collected by DELPHI in 1995 and 1996 at the center of mass energies of 133, 161 and 172 GeV. No evidence of these processes was found for a decay length ranging from ~ 1 mm to ~ 20 cm and limits were derived on $m_{\tilde{\tau}}$ and $m_{\tilde{G}}$.

1 Introduction

Among the theoretical extensions of the Standard Model (SM), Supersymmetry (SUSY) is at present the possibility which most focuses the attention of both theoreticians and experimentalists. The main reasons for this success are: i) SUSY incorporates gravity, thus allowing for unification of the three SM gauge couplings; ii) SUSY justifies the existence of a light Higgs boson at the electroweak scale, provided that the supersymmetric partners of the SM particles have masses < 1 TeV.

However no final agreement has been reached so far concerning the SUSY breaking mechanism. Within traditional models, SUSY breaking is mediated by gravity in a hidden sector and it takes place at a scale of order 10^{11} GeV.

Some other models [1], instead, predict a low energy SUSY breaking at a scale of ~ 100 TeV, mediated by SM gauge interactions. The main advantage of these Minimal Gauge Mediated SUSY Breaking (MGMSB) models is that they have a fewer free parameters and a higher degree of predictivity.

In particular, the mass spectrum of the supersymmetric particles can be derived from the ratio $\Lambda = F/M$, where F is the squared scale of the SUSY breaking and M the mass of the messenger. In order to get masses < 1 TeV, Λ should not exceed ~ 100 TeV.

In the MGMSB models the Lightest Supersymmetric Particle (LSP) is the gravitino ($\tilde{G}$). Therefore, if R parity is conserved, every decay chain involving supersymmetric particles should end up with the production of a gravitino.

The gravitino mass $m_{\tilde{G}}$ is determined by F, through the relation [2]

$$m_{\tilde{G}} = \frac{F}{\sqrt{3}M} = 5.9 \cdot 10^{-5} \left(\frac{F}{(500GeV)^2}\right) \text{eV}$$

where $M = (8\pi G_{Newton})^{-1/2}$. The dependence of $M_{\tilde{G}}$ on $\sqrt{F}$ is shown in fig.1.

The gravitino mass is bounded by cosmological constraints [3] to be $<\sim 10^4$ eV. On the other hand, the necessity to avoid R-axions in MGMSB models [4] is in favour of $m_{\tilde{G}} >\sim 1$ eV.

The Next to LSP (NLSP) is often considered to be a neutralino. In this case one would expect the dominant SUSY process at LEP to be $e^+e^- \to \tilde{\chi}_1^0\tilde{\chi}_1^0$, with each $\tilde{\chi}_1^0$ decaying into $\tilde{G}\gamma$.

However, for large values of tan β (the ratio between the two vacuum expectation values of the Higgs fields), the mixing between $\tilde{\tau}_R$ and $\tilde{\tau}_L$ could give rise to a $\tilde{\tau}_1$ lighter than the lightest neutralino. In this scenario the $\tilde{\tau}_1$ would be the NLSP and the dominant SUSY process would be $e^+e^- \to \tilde{\tau}_1^+\tilde{\tau}_1^-$, with $\tilde{\tau}_1 \to \tau\tilde{G}$.

The theoretical cross sections for $\tilde{\tau}\tilde{\tau}$ production, computed by the program Susygen [5], are shown in fig. 2 as a function of the $\tilde{\tau}$ mass.

The $\tilde{\tau}$ lifetime depends on the SUSY breaking scale, as shown in fig.1, therefore it increases with increasing $\tilde{G}$ mass, whilst it decreases with increasing $\tilde{\tau}$ mass.

In this analysis we have considered $\sqrt{F}$ ranging from ~ 100 to ~ 350 TeV. If we assume Λ=100 TeV, this implies a messenger scale between 100 and ~ 1200 TeV. The corresponding values of the gravitino mass are below ~ 20 eV, and the proper $\tilde{\tau}$ life time multiplied by the speed of light is shorter than ~ 20 cm (see fig.1).

At LEP, a large fraction of these decays take place within the beam pipe, therefore they may be observed by searching for events with low multiplicity, high missing energy and missing momentum (due to the gravitinos and the neutrinos produced in the decay

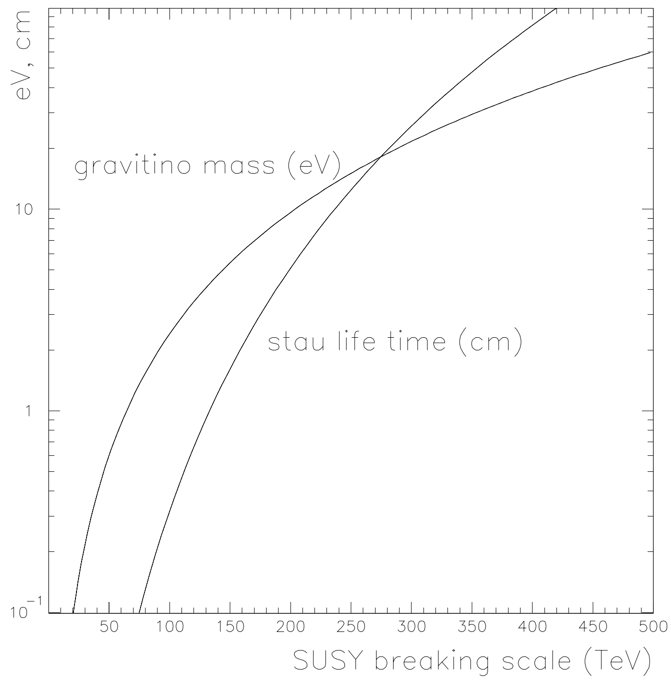

Figure 1: $\tilde{G}$ mass as a function of the the SUSY breaking scale. The $\tilde{\tau}$ life time dependence on the same parameter is also shown, for M$_{\tilde{\tau}}$=50 GeV.

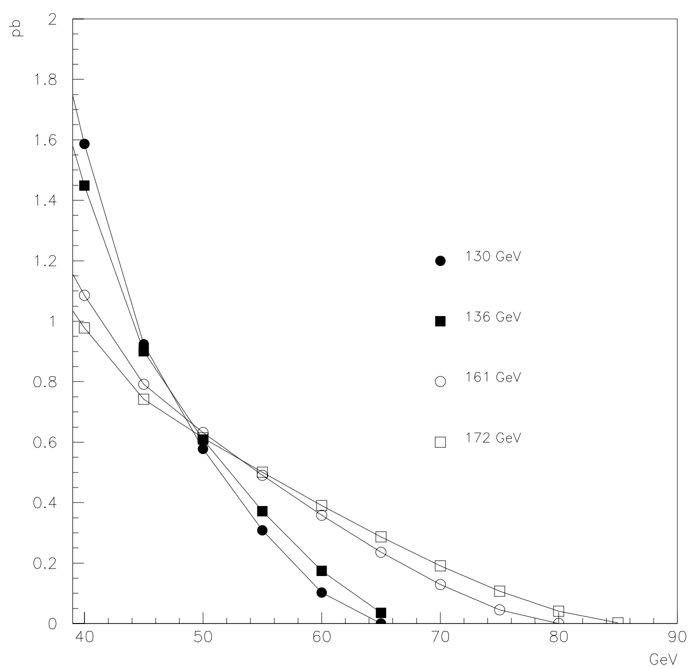

Figure 2: Theoretical cross section for $\tilde{\tau}\tilde{\tau}$ production as a function of $\tilde{\tau}$ mass.

chain), and large impact parameters of the leading tracks.

For larger values of the gravitino mass, i.e. for longer $\tilde{\tau}$ decay lengths, different experimental techniques have been used to search for this decay within the DELPHI experiment. For decays happening within the tracking volume of the detector, a signal is expected to show up as a sudden bending ("kink") of the track, due to the emission of the invisible gravitino [6]; when the decay length is still longer, the $\tilde{\tau}$ may go through the whole detector before decaying and may be recognized using the particle identification tools based on specific ionization in the TPC and on the RICH information [7].

The data used are those collected by DELPHI in the 1995 and 1996 high energy runs at 130, 136, 161 and 172 GeV.

2 Simulation studies and analysis procedure

In order to determine the efficiency corresponding to each combination of $M_{\tilde{\tau}}$ and $M_{\tilde{G}}$ at each center of mass energy, 21 sets of Monte Carlo (MC) signal events were generated with the SUSYGEN program [5] taking into account the radiative corrections. They were then passed through the detailed simulation of the DELPHI detector [8] and through the reconstruction program used for the real data [9]. $M_{\tilde{\tau}}$ ranged from 40 to 65 GeV and $M_{\tilde{G}}$ from 1 to 30 eV, as shown in tab.1 where t is the proper $\tilde{\tau}$ lifetime and $\beta\gamma ct$ is its decay length in the lab system.

The background study is based on samples of $\gamma\gamma$, γZ^o, Bhabha, eeZ^o and Compton events, generated at the relevant E_{CM} energies and passed through the full detector simulation. Above the production threshold, also the WW events contribute to the background, especially in the channel WW $\rightarrow \tau\tau$ which has a topology similar to the signal searched for and can only be reduced by a cut on the impact parameters.

The analysis starts with a loose track selection, based on momentum ($\geq$ 400 MeV), momentum error ($\leq$ 100 %), polar angle ($\geq 20^o$), track length ($\geq$ 30 cm), and impact parameter ($\leq$ 10 cm on the RΦ plane, $\leq$ 15 cm along z). All the neutrals $\geq$ 100 MeV are accepted. Any calorimetric deposit associated to a discarded charged tracks is kept as a neutral track.

The event thrust direction is determined using the selected tracks, the event is then divided in two hemispheres by the plane normal to the thrust axis and the most energetic track in each hemisphere is found. These tracks are named in the following "leading tracks" (l.t.1, l.t.2).

The set of cuts adopted is as follows:

- $2 \leq$ number of charged tracks ≤ 4
- Radius of first measured point of l.t.1 and l.t.2 on the RΦ plane $\leq$ 50 cm
- $|p_{l.t.1} - p_{l.t.2}| \leq 95\%$ of the total charged energy
- At least one l.t. has a track segment in the TPC
- Both l.t.'s have at least one track segment beyond the ID
- Both tracks out of HPC theta cracks
- Visible energy of the event between 8% and 70% of the center of mass energy

- Transverse missing momentum ≥ 0.03 center of mass energy (1)
- Polar angle of missing momentum within $[30^o,150^o]$ (2)
- Total energy within the two cones of 30^o around the beam ≤ 0.1 visible energy (3)
- neutral energy ≤ 0.35 beam energy (4)
- Angle between the l.t.'s in the RΦ plane ≤ 3 rad (5)
- Acolinearity $\geq 10^o$ (6)
- $\sqrt{p^2_{l.t.1} + p^2_{l.t.2}} \geq 0.06$ beam energy (7)
- Electromagnetic energy (l.t.1) + electromagnetic energy (l.t.2) ≤ 0.7 beam energy (8)
- $\sqrt{i.p.^2_{l.t.1} + i.p.^2_{l.t.2}} \geq 0.06$ cm (9)

Table 1. Samples of signal events and corresponding efficiencies

E_{CM} (GeV)	$M_{\tilde{\tau}}$ (GeV)	$M_{\tilde{G}}$ (eV)	ct (cm)	$\beta\gamma ct$ (cm)	$\epsilon(\%)$
130	40	0.7	0.075	0.083	12 ± 1
	50	15.0	12.38	9.87	23 ± 1
	60	15.0	4.97	1.99	40 ± 2
161	40	5.4	4.91	7.58	29 ± 1
	50	1.3	0.093	0.12	20 ± 1
		1.7	0.16	0.19	24.0 ± 0.9
		3.8	0.81	0.97	35 ± 1
	60	14.1	4.39	3.79	37 ± 1
		30.0	19.87	17.13	15 ± 1
172	40	6.4	6.90	11.83	21 ± 1
	50	1.7	0.16	0.21	26.3 ± 0.9
		3.8	0.81	1.08	35 ± 1
		7.4	3.01	4.02	35 ± 1
		10.4	5.95	8.04	25 ± 1
	60	1.7	0.064	0.063	11.3 ± 0.5
		3.8	0.32	0.32	30.5 ± 0.7
		10.6	2.48	2.47	38 ± 1
		20.7	9.46	9.38	23 ± 1
	65	1.8	0.05	0.042	4.7 ± 0.7
		11.6	1.99	1.67	38 ± 1
		17.4	4.48	3.76	36 ± 1

Cuts 1-3 aim to reject the $\gamma\gamma$ events; cuts 4-9 suppress the background due to standard $e^+e^- \to f\bar{f}$ processes; cuts 5 and 6 also suppress the cosmic background. Cut 9 reduces the standard $\tau\tau$ events from Z^o and WW, it is applied to the RΦ projections of the impact parameters. As an example, figure 3 shows the distribution of $\sqrt{i.p._{l.t.1}^2 + i.p._{l.t.2}^2}$ at 172 GeV, for $\gamma Z^o \to \tau\tau$ events, and for signal events with $m_{\tilde{\tau}} = 50$ GeV and a mean decay length in the lab system of 2.1 mm.

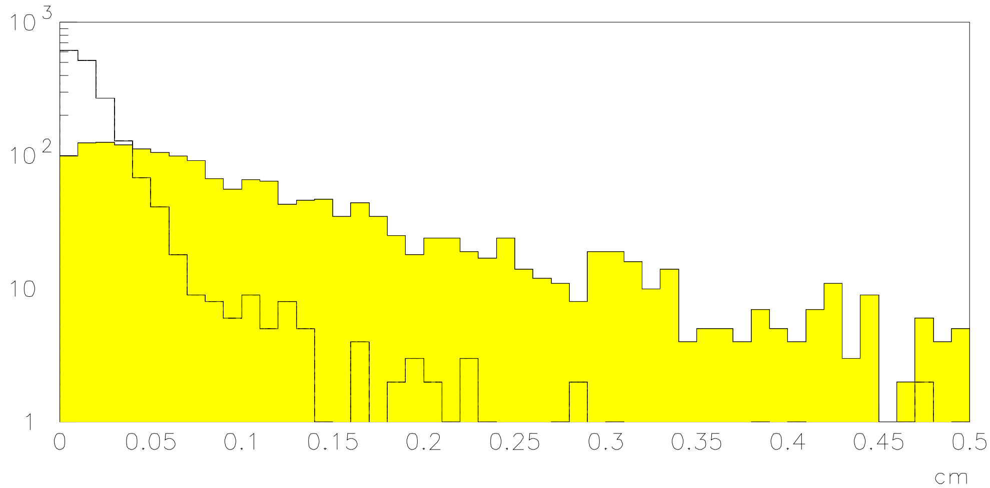

Figure 3: Squared sum of the l.t. impact parameters, for standard $\gamma Z^o \to \tau\tau$ events and for $\tilde{\tau}\tilde{\tau}$ events (shaded) with $m_{\tilde{\tau}} = 50$ GeV, E$_{CM}$ = 172 GeV, $\beta\gamma ct = 2.1$ mm

3 Efficiency and background study

From the application of the above cuts to the MC signal events, it turns out that the efficiency does not depend separately on the center of mass energy and on the $\tilde{\tau}$ mass but rather on the $\tilde{\tau}$ decay length in the lab. system, which is determined by both these variables. Figure 4 shows the efficiency as a function of the $\tilde{\tau}$ decay length for the various simulated energies; the $\tilde{\tau}$ mass values are shown in tab.1.

Cut 9 is the cause of the efficiency drop at small decay lengths, whilst at large decay lengths the loss of efficiency is due to the upper impact parameter cut used in the track selection.

The application of the same set of cuts to the background MC events allows an estimate of the expected background. The non negligible contributions are shown in tab.2. They are normalized to the integrated luminosities of the three samples.

As expected, the main sources of background come from the channels with τ's. The contributions from WW events are small, owing to the cross section.

The selected MC background events were checked through a visual scan using the graphic analysis program DELGRA [10].

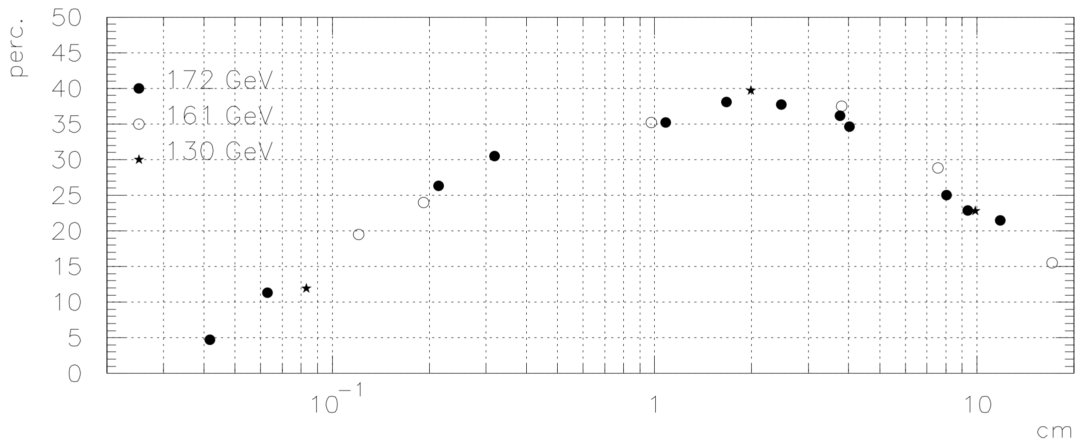

Figure 4: Selection efficiency versus the $\tilde{\tau}$ decay length in the lab. system.

Table 2: Expected background events

channel	130+136 GeV	161 GeV	172 GeV
$\gamma\gamma \rightarrow \tau\tau$	$0^{+0.75}_{-0}$	0.09 ± 0.09	0.08 ± 0.08
$\gamma Z^o \rightarrow \tau\tau$	0.22 ± 0.11	0.21 ± 0.12	0.07 ± 0.05
WW	-	0.028 ± 0.009	0.12 ± 0.04
$ee\tau\tau$	0.08 ± 0.08	0.16 ± 0.16	$0^{+0.06}_{-0}$
	$0.30^{+0.76}_{-0.14}$	0.49 ± 0.22	$0.27^{+0.12}_{-0.10}$

4 Results

The selection criteria described in section 2 were applied to the 4 sets of data taken at 172 ($\sim 10pb^-1$), 161 ($\sim 10pb^-1$), 136 ($\sim 3.1pb^-1$) and 130 ($\sim 2.9pb^-1$) GeV. Only 1 event survived the cuts: it was visually studied in detail with DELGRA and it turned out to be a cosmic event where one of the two branches was badly measured ($\Delta E/E = 4$) and hence discarded, whilst a soft extra track caused the event to be selected. Therefore it was not considered as a candidate.

In order to determine the exclusion areas on the plane $\mathrm{M}_{\tilde{G}}$ $\mathrm{M}_{\tilde{\tau}}$, for each pair of $M_{\tilde{\tau}}$ $M_{\tilde{G}}$ values first the proper $\tilde{\tau}$ life time is computed. Then the following calculations are repeated for each center of mass energy: the mean $\tilde{\tau}$ momentum is obtained from the MC taking into account the initial state radiation and it is used to determine the $\tilde{\tau}$ decay length in the laboratory; the corresponding efficiency is derived interpolating the data shown in fig.4; the cross section is computed as in fig. 1 and the number of expected events is determined. The total number of expected events within all the available data sets is finally compared with the upper limits corresponding to 0 candidates, at 90 and 95% confidence level: the points where this number exceeds the upper limit are excluded.

The results are shown in fig. 5.

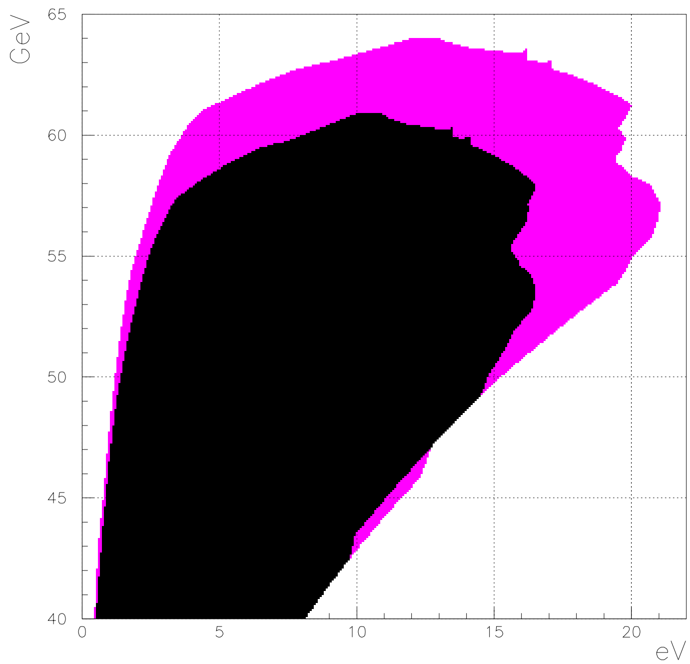

Figure 5: Exclusion plot at 95% and 90% confidence level, in the plane $M_{\tilde{\tau}}$ $M_{\tilde{G}}$

5 Conclusions

A search for the process $e^+e^- \to \tilde{\tau}\tilde{\tau} \to \tau\tilde{G}\tau\tilde{G}$ within the framework of MGMSB, was performed using the data collected by DELPHI at LEP in 1995-1996. No candidate was found within the data at 130-136, 161 and 172 GeV for a total luminosity of ~ 26 pb^{-1}. Intervals of m$_{\tilde{G}}$ were excluded for m$\tilde{\tau} < 61$ GeV at 95% C.L.: e.g. for m$\tilde{\tau} = 50$ (55) GeV, gravitino masses between 1.3 (2.3) and 14.8 (15.8) were excluded.

References

[1] see for example:

M. Dine, W. Fischler and M. Srednicki, Nucl. Phys. B189 (1981) 575

S. Dimopoulos and S. Raby, Nucl. Phys. B192 (1981) 353

M. Dine and W. Fischler, Phys. Lett. B110 (1982) 227

M. Dine and M. Srednicki, Nucl. Phys. B202 (1982) 238

L. Alvarez-Gaumè , M. Claudson and M. Wise, Nucl. Phys. B207 (1982) 96

C. Nappi and B. Ovrut, Phys. Lett. B113 (1982) 175

M. Dine and W. Fischler, Nucl. Phys. B204 (1982) 346

S. Dimopoulos and S. Raby, Nucl. Phys. B219 (1983) 479

and the more recent contributions:

M. Dine and A. E. Nelson, Phys. Rev. D48 (1993) 1277

M. Dine, A. E. Nelson and Y. Shirman, Phys. Rev. D51 (1995) 1362

M. Dine, A. E. Nelson, Y. Nir and Y. Shirman, Phys. Rev. D53 (1996) 2658

S. Dimopoulos, M. Dine, S. Raby and S. Thomas, Phys. Rev. Lett. 76 (1996) 3494

[2] S. Ambrosanio, G. L. Kane, G. D. Kribs, S. P. Martin, S. Mrenna, Phys. Rev. D54 (1996) 5395

[3] H. Pagels and J. R. Primack, Phys. Rev. Lett. 48 (1982) 223

T. Moroi, H. Murayama and M. Yamaguchi, Phys. Lett. B303 (1993) 289

[4] A. E. Nelson and N. Seiberg, Nucl. Phys. B416 (1994) 46

J. Bagger, E. Poppitz and L. Randall, Nucl. Phys. B426 (1994) 3

[5] CERN 96-01, vol.2. See also the SUSYGEN manual, by S. Katsanevas and P. Morawitz, in http://lyohp5.in2p3.fr/delphi/katsan/susygen.html

[6] Contribution to HEP'97, paper n.350.

[7] P.Abreu et al., Phys. Lett. B396 (1997) 315

[8] DELPHI 89-68, PROG 143

[9] DELPHI 89-44, PROG 137

[10] DELGRA manual 1.0 in: http://wwwcn.cern.ch/ delgra/